Microstructure and properties of Nb/Ta multilayer films irradiated by a high current pulse electron beam*

Ma Xin-Xin(马欣新)[a)b)], Guo Guang-Wei(郭光伟)[a)c)], Tang Guang-Ze(唐光泽)[d)†], Sun Ming-Ren(孙明仁)[b)], and Wang Li-Qin(王黎钦)[e)]

[a)] State Key Laboratory of Advanced Welding and Joining, Harbin Institute of Technology, Harbin 150001, China
[b)] National Key Laboratory of Science and Technology on Precision Hot Processing of Metals, Harbin Institute of Technology, Harbin 150001, China
[c)] Key Laboratory on Materials Behavior & Evaluation Technology in Space Environment, Harbin Institute of Technology, Harbin 150001, China
[d)] School of Mechanical Science and Engineering, Northeast Petroleum University, Daqing 163318, China
[e)] School of Mechatronics Engineering, Harbin Institute of Technology, Harbin 150001, China

(Received 26 June 2012; revised manuscript received 10 January 2013)

Nb/Ta multilayer films deposited on Ti6Al4V substrate with Nb and Ta monolayer thicknesses of 30 nm, 120 nm, and 240 nm were irradiated by a high current pulse electron beam (HCPEB) to prepare Nb–Ta alloyed layers. The microstructure and the composition of the outmost surface of melted alloyed layers were investigated using a transmission electron microscope (TEM) equipped with an X-ray energy dispersive spectrometer (EDS) attachment. The Ta content of the alloyed surface layer prepared from the monolayer of thickness 30 nm, 120 nm, and 240 nm was ∼ 27.7 at.%, 6.37 at.%, and 0 at.%, respectively. It was found that the Ta content in the alloyed layer plays a dominant role in the microstructure of the films. The hardness and the wear rate of the alloyed layers decrease with the increasing content of Ta in the surface layer.

Keywords: Nb–Ta alloyed layer, multilayer film, high current pulse electron beam, wear resistance

PACS: 62.20.Qp, 68.37.Lp, 68.55.Nq, 68.65.Ac **DOI:** 10.1088/1674-1056/22/5/056202

1. Introduction

Ti6Al4V alloy is widely used in the field of biomedicine, such as hip stems in total hip replacement, dental devices, and bone pegs. However, the properties of this alloy make it still far from being a perfect implant material. For example, the release of Al and V ions in the human environment will cause cell inflammation, and the wear resistance still needs further improvement.

Surface alloying is an effective way to improve the properties of Ti6Al4V. Research[1–3] has shown that Ta and Nb elements are beneficial to form a stable passive film in corrosion media, which greatly reduces the corrosion rate of the alloy. Li *et al*. reported that the formation of Nb_2O_5 during the wear process can obviously reduce the wear rate of the alloy.[4] Besides the good wear and corrosion resistance, Ta and Nb elements also show excellent biocompatibility in the human body.[5,6] High current pulse electron beam (HCPEB) irradiation can eliminate the interface between substrate and coated layer to solve the peeling-off problem, which has great advantages for implants.

In this paper, Nb/Ta multilayer films were pre-deposited on Ti6Al4V substrates and then irradiated by HCPEB. The dependence of microstructure on the Ta content and the influence of microstructure on the properties of the surface alloyed layers are discussed.

2. Experiment

It is well known that an alloy's microstructure strongly depends on its composition. The calculation result of Rotshtein *et al*. showed that the diffusion distance of atoms is ∼ 100 nm after 1 pulse irradiation.[7] In order to investigate the relationship between the structure and the Nb–Ta alloy composition after HCPEB treatment, Nb/Ta multilayer films with monolayer thicknesses of 30 nm, 120 nm, and 240 nm were prepared by direct-current magnetron sputtering, in which Ta and Nb monolayers were deposited alternatively on ϕ30 mm×5 mm Ti6Al4V substrates with no cooling. The deposition processes were carried out in a JGP560 high vacuum multi-function magnetron sputtering system. Two 2-inch magnetron targets made of Ta (99.99 wt.%) and Nb (99.99 wt.%), respectively, were installed inside the chamber. The samples could be moved to face each target and deposited for a certain time to achieve the desirable monolayer thickness. The distance between target and substrate was 50 mm. The background pressure was less than 6×10^{-4} Pa, and the work pressure was about 1.3 Pa with 99.99 wt.% Ar gas. During the Nb/Ta multilayer films preparation, a −150 V bias was applied to the samples, and the target powers of Ta and Nb were 75 W and 48 W, respectively, the corresponding depositing rates of Ta and Nb films were about 0.25 nm/s and 0.21 nm/s, respectively.

*Project supported by the National Basic Research Program of China (Grant No. 2013CB632305), the Guangdong Province University-Industry Cooperation Project of the Ministry of Education, China (Grant No. 2010B090400444), the Guangdong International Cooperation Projects, China (Grant No. 2010B050900003), and the Guangdong Science and Technology Plan Projects, China (Grant No. 2010A070500002).

†Corresponding author. E-mail: oaktang@hit.edu.cn

© 2013 Chinese Physical Society and IOP Publishing Ltd

Table 1. Technological parameters of Nb/Ta multilayer film deposition.

Sample group No.	Monolayer thickness/nm	Monolayer depositing time for Ta/s	Monolayer depositing time for Nb/s	Multilayer period	Multilayer thickness/nm
1	30	122	148	15	900
2	120	488	592	15	3600
3	240	976	1184	15	7200

The Nb/Ta multilayer films preparation technological parameters are presented in Table 1, and the outmost layer is Nb.

After 15 periods of the above-mentioned multilayer films deposition, for sample groups 1–3, the corresponding total thicknesses were 900 nm, 3600 nm, and 7200 nm with initial hardness of 6.64 GPa, 3.61 GPa, and 2.09 GPa at the depth of 100 nm, respectively.

HCPEB irradiation was carried out using a Nadezhda-2 electron beam source.[8] The base pressure was $\sim 10^{-4}$ Pa, and the working gas was argon with pressure 3×10^{-2} Pa. The pulse duty on time was 2.6 μs, the acceleration voltage was 33 kV, and the energy density of one pulse shot was ~ 5 J/cm^2. In this experiment, 1 pulse irradiation was used.

A JEM-2100 type transmission electron microscope (TEM) with an X-ray energy dispersive spectrometer (EDS) attachment was employed to analyze the surface microstructure and the composition of the irradiated layer to gain an insight into the effect of the composition on the microstructure of the irradiated layer. The samples adopted in the surface structural observation were prepared as follows. Firstly, the sample plate with the thickness of ~ 200 μm was spark-cut from the irradiated sample, paralleled to the surface; then, mechanical polishing was implemented to thin the plate down to ~ 50 μm from the opposite side of the irradiation surface; lastly, ion etching from the opposite side of the irradiation surface was performed.

The hardness of the irradiated layer was measured by nano-indentation testing using a nano-indenter XP instrument (Agilent Company) in continuous stiffness measurement (CSM) mode.[9] Six tests were performed for each sample to obtain the average hardness. The hardness at the depth of 100 nm was used to characterize the alloyed layers.

For the purpose of evaluating the wear resistance of the alloyed surface, the dry-sliding friction test was exerted against a $\phi 6$ mm ZrO_2 ball by using a pin-on-disk tester. The applied load was 0.5 N, the slide speed was 0.06 m/s with total sliding distance of 188.4 m. The wear rate was defined as

$$W = \frac{\Delta V}{LD} = \frac{S\Delta l}{LD}, \tag{1}$$

where ΔV is the volume of the wear track; S is the area of the wear track cross-section; Δl is the length of the wear track; D is the sliding distance, and L is the applied load in the test. The area of the wear track cross-section of the sample was measured by a profile meter.

3. Results

Figure 1 shows the microstructure in the outmost surface of the alloyed layer from the Ta and Nb monolayer of thickness 30 nm. In Fig. 1(a), fine crystal grains with size ranging from 30 nm to 100 nm are found, and the boundary between the grains is hard to distinguish. The EDS result reveals that the Ta content in this zone is ~ 27.7 at.%, as shown in Fig. 1(d). The HRTEM image and the corresponding amorphous dot and diffraction circles shown in Fig. 1(b) for zone B in Fig. 1(a) indicate that this zone is amorphous and consists of nano-crystals. Figure 1(c) is the HETRM image of zone C in Fig. 1(a). The amorphous zones in Fig. 1(c) are smaller compared with those in Fig. 1(b), and the insert reveals that the nucleus size is several nanometers.

Figure 2(a) shows the grain morphology of surface layer from the Ta and Nb monolayer of thickness 120 nm. The grain size ranges from 100 nm to 500 nm. Compared with Fig. 1(a), the grain boundary can be clearly distinguished. The dislocation tangle is observed in some grains, such as grains A and B. The weak aimless speckle around the central transmission spot in the insert, displaying a small diffraction pattern, indicates that there still exists amorphous zones in the alloyed layer. The Ta content in the grains is 6.37 at.% from the EDS measurement, as shown in Fig. 2(c). Figure 2(b) shows the image of the stacking faults with width of ~ 50 nm. The kinking in the stacking fault, which is in the black circle, is believed to be the trace of shear deformation.

The surface microstructure of the alloyed layer from the Ta and Nb monolayer of 240 nm is exhibited in Fig. 3(a). It is found that the grain size is close to 500 nm. Some cavities with diameter of several tens nanometers exist at the grain boundaries. Because the initial thickness of the Ta and Nb monolayer is 240 nm, which is thicker than the diffusion distance of Ta atoms after 1 pulse irradiation, it is justifiable that the surface layer should be only composed of only the Nb element. Figure 3(b) is the enlarged image of Fig. 3(a), and the insert is the corresponding diffraction patterns. Both the EDS testing result and the index of the diffraction pattern, displayed in Figs. 3(b) and 3(c), confirm that the surface of the alloyed layer is pure Nb without Ta. No amorphous spot is observed in Fig. 3(b).

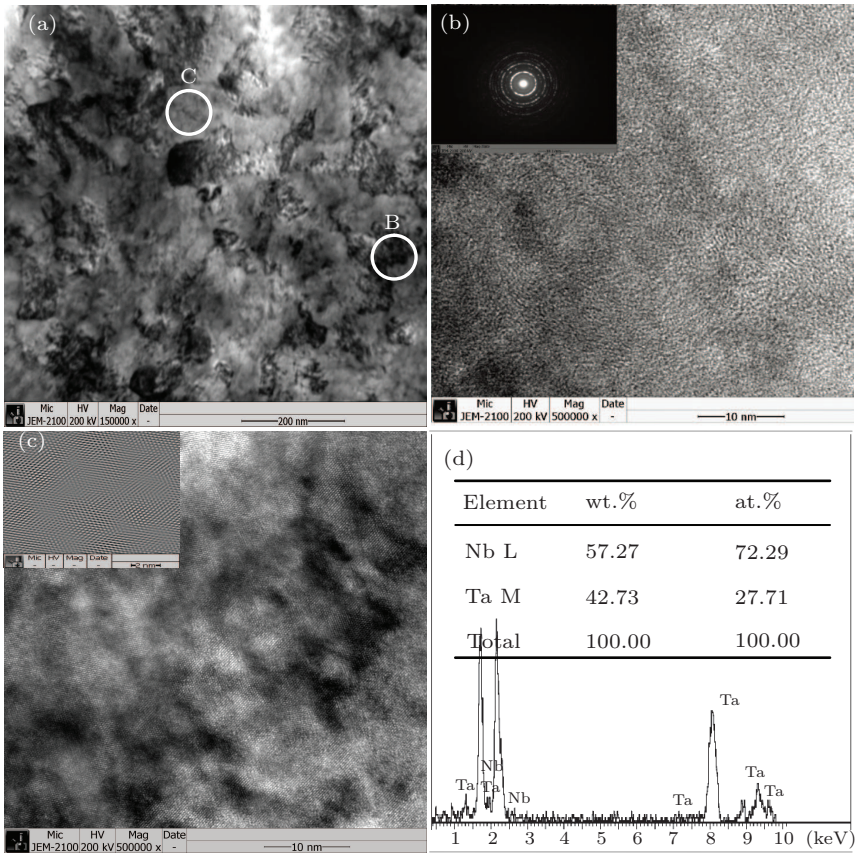


Fig. 1. TEM images and EDS results of the alloyed layer from Ta and the Nb monolayer of 30 nm: (a) TEM image, (b) HRTEM and corresponding diffraction patterns (insert) of zone B, (c) HRTEM of zone C, the insert reveals the size of the nucleus, (d) EDS pattern.

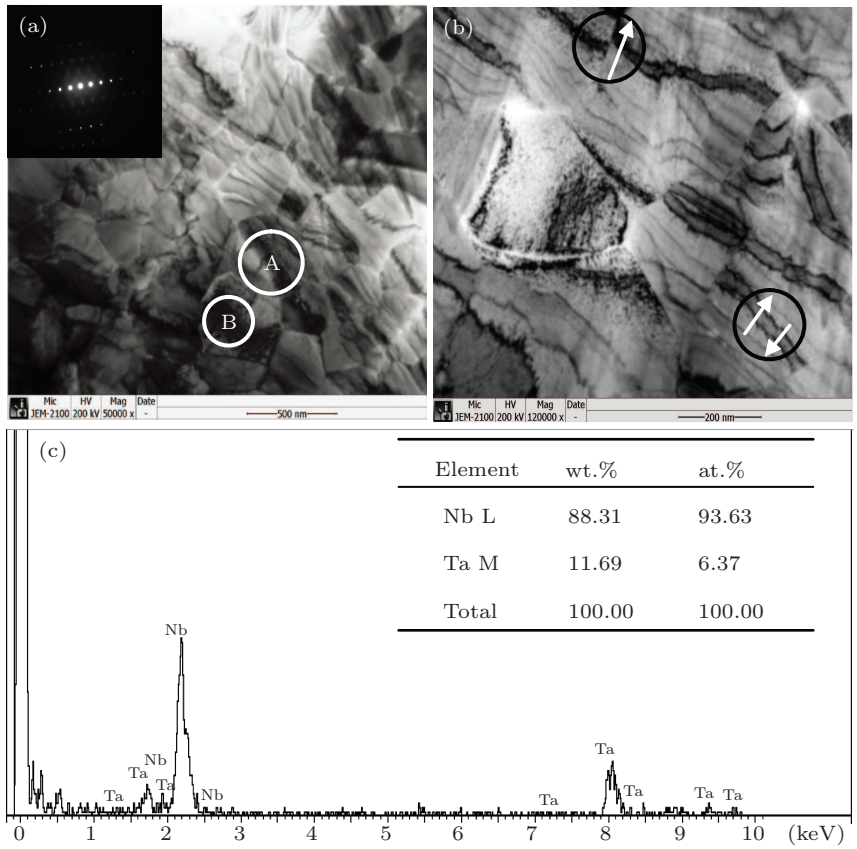
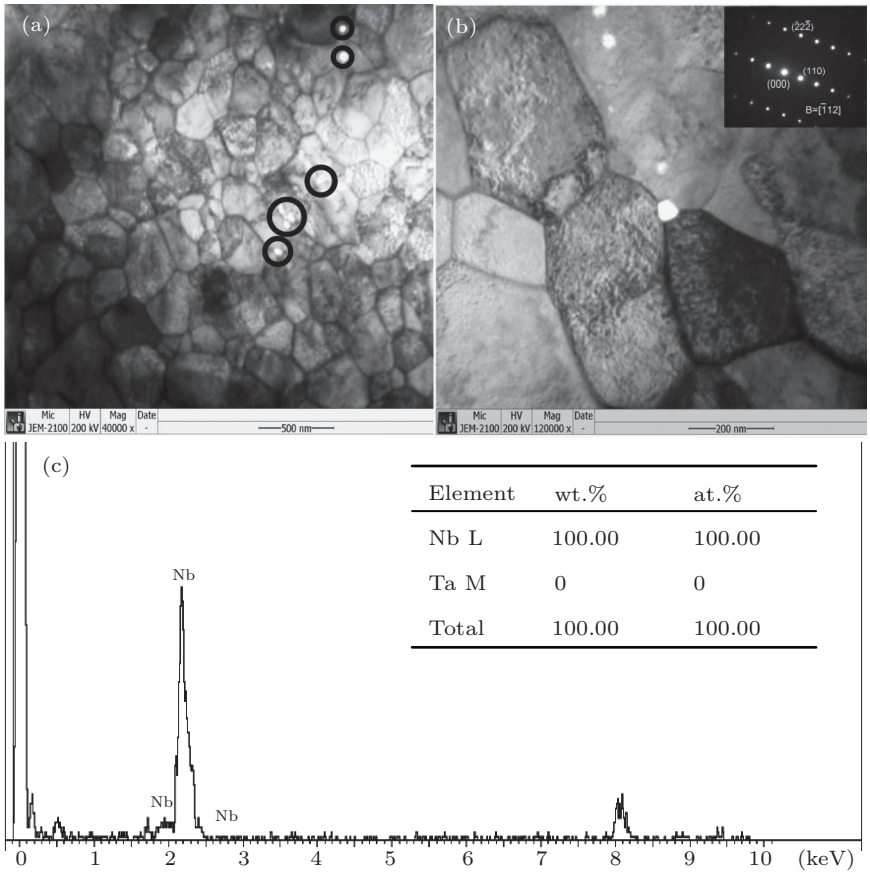


Fig. 2. TEM images and EDS results of the alloyed layer from Ta and the Nb monolayer of 120 nm: (a) TEM image and corresponding patterns (insert), (b) image of the stacking fault, (c) EDS pattern.



Element	wt.%	at.%
Nb L	100.00	100.00
Ta M	0	0
Total	100.00	100.00

Fig. 3. TEM images and EDS results of the alloyed layer from Ta and the Nb monolayer of 240 nm: (a) TEM morphology, (b) enlarged morphology and the corresponding diffraction pattern (insert), (c) EDS pattern.

Figures 4(a) and 4(b) give the testing results of the hardness and the wear rate of HCPEB alloyed layers with various monolayer thicknesses. The hardness of the alloyed layer with a monolayer thickness of 30 nm reaches 7.56 GPa, about 2 GPa higher than the Ti6Al4V substrate. With the increase of the monolayer thickness, the hardness of the alloyed layer reduces. The wear rate of the alloyed layer with a monolayer thickness of 30 nm is just a fifteenth of the substrate. The wear resistance of the alloyed layer decreases as the monolayer thickness increases.

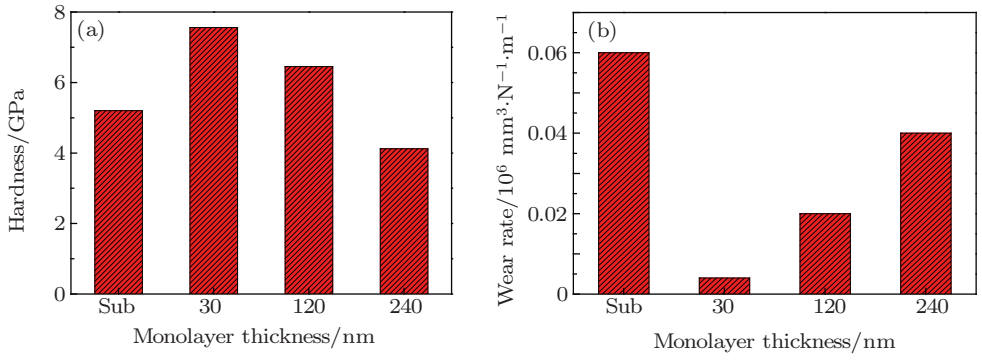


Fig. 4. (color online) (a) Hardness and (b) wear rate of alloyed layers and substrate.

4. Discussion

According to the above results, three typical alloyed surface layers with different Ta contents are prepared. It is found that the structure of the Nb–Ta alloyed layer prepared from the HCPEB treatment of Nb/Ta multilayer films greatly depends on the Ta content. The grain size increases with the Ta content decreasing. The amorphous structure is easier to form in the alloy with a high Ta content. The dislocation tangle and the stacking fault are found when the Ta content reduces to 6.37 at.%. No amorphous structure is observed in the pure Nb

layer, and there are fewer crystal defects in the grains.

The superfast cooling process is the main dynamic factor determining the microstructure of the Nb–Ta alloyed layers. According to the Nb–Ta binary alloy phase diagram, the atom diffusion is necessary when the crystal nuclei separate out and grow from the melt. Because the solidification time of the melt is very short, about several microseconds, the diffusion distance of atoms is limited. As a result, the crystal nucleation and the growth of grains with a high Ta content are restricted to small grains. For the pure Nb melt, the long distance diffusion of atoms is not needed for the crystal nucleation and growth, thus the average grain size is the largest in the irradiated layers.

The superfast cooling process also causes the compositional supercooling of the alloy melt. The degree of supercooling of the alloy melt with a higher Ta content is also higher. The melt solidification at high supercooling tends to form an amorphous structure because of the low atom migration rate. When the Ta content declines to 6.37 at.%, the degree of supercooling of the alloy melt reduces. The crystal defects in this alloy are mainly composed of dislocation tangles and stacking faults. The degree of supercooling of the Nb melt should be the lowest; and the amount of crystal defects is the lowest.

The alloyed layer from a 30 nm monolayer has a high Ta content with smaller crystal size, larger amorphous zone, and more crystal defects. The material strengthening theory indicates that such a structure should have a higher hardness. The alloyed layers prepared from 120 and 240 nm monolayers show mixture structures in depth and have a sub-layer with low hardness, where the crystal size is larger, the amount of amorphous zones and crystal defects is lower than that of the alloyed layer with a higher Ta content. As a result, the total hardness of these two alloyed layers is lower.

The wear rate of dry sliding friction strongly depends on the material hardness and the nature of the oxide layer formed in the dry sliding friction test.[10] Compared with Ti6Al4V alloy, the oxides of Ta and Nb can both act as a solid lubrication film during a dry friction test to greatly reduce the wear rate. The alloyed layer from the 30 nm monolayer has the lowest wear rate among the three surface layers resulting from its highest hardness.

5. Conclusion

The microstructure and the wear resistance of Nb–Ta alloyed layers prepared from HCPEB irradiating Nb/Ta multilayer films were investigated. The structure of the Nb–Ta alloyed layer predominantly depends on the Ta content. The grain size increases with the Ta content decreasing. The alloyed layer with a higher Ta content has more amorphous structures. The dislocation tangle and the stacking fault are the main crystal defects for the alloyed layer with Ta content of 6.37 at.%. For the pure Nb grains, no amorphous structure is observed, and there are fewer crystal defects in the grain. The alloyed layer from the 30 nm monolayer shows the highest hardness and the lowest wear rate.

References

[1] Karayan A I, Park S W and Lee K M 2008 *Materials Letters* **62** 1843

[2] Maeng S M, Axe L, Tyson T A, Gladczuk L and Sosnowski M 2006 *Surface & Coatings Technology* **200** 5717

[3] Metikoš –Huković M, Kwokal A and Piljac J 2003 *Biomaterials* **24** 3765

[4] Li S J, Yang R, Li S, Hao Y L, Cui Y Y, Niinomi M and Guo Z X 2004 *Wear* **257** 869

[5] Zhou Y L, Niinomi M, Akahori T, Fukui H and Tod H 2005 *Materials Science and Engineering A* **398** 28

[6] Niinomi M, Kuroda D, Fukunaga K, Morinaga M, Kato Y, Yashiro T and Suzuki A 1999 *Materials Science and Engineering A* **263** 193

[7] Rotshtein V P, Ivano Yu F, Markov A B, Proskurovsky D I, Karlik K V, Oskomov K V, Uglov B V, Kuleshov A K, Novitskaya M V, Dub S N, Pauleau Y and Shulepov I A 2006 *Surface & Coatings Technology* **200** 6378

[8] Guan Q F, Zou H, Zou G T, Wu A M, Hao S Z, Zou J X, Qin Y, Dong C and Zhang Q Y 2005 *Surface & Coatings Technology* **196** 145

[9] Li X D and Bhushan B 2002 *Materials Characterization* **48** 11

[10] Quinn T F J 1983 *NASA Contractor Report* 3686